

# Contact Lens Detection using Local Phase Quantization and Binary Gabor Pattern

Lovish

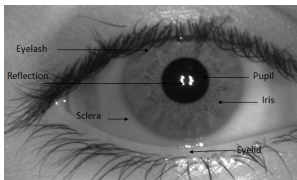
Supervisor: Dr. Phalguni Gupta

Department of Computer Science and Engineering  
Indian Institute of Technology Kanpur

Feb 5, 2015

# Problem Statement

- Biometrics - Face, Fingerprint, Palmprint, Ear, Iris
- Iris
  - Part between pupil and sclera
  - Unique for every individual [1]
  - Resistant to circumvention

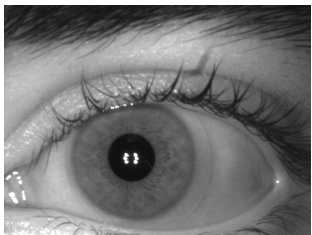


(a) Iris structure

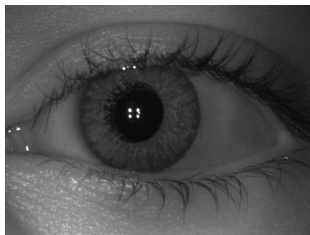
Figure 1: Human Iris Anatomy

# Problem Statement

- Recent increase in use of Contact lenses
  - Soft Contact Lenses
    - Transparent
    - Specular reflection
  - Cosmetic Lenses
    - Part Opaque and part transparent
    - Artifacts over iris pattern



(a) Transparent Contact Lens

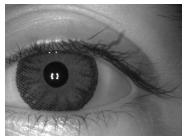


(b) Cosmetic Contact Lens

Figure 2: Type of Contact Lens

# Problem Statement

- Cosmetic Lenses
  - Differ in color, printed pattern, material



(a) OxyColor



(b) Flamboyent



(c) O2Max

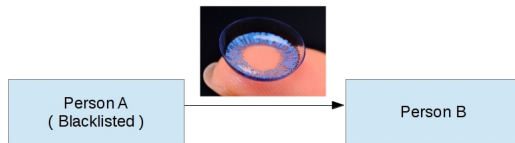


(d) Freshlook [2]

Figure 3: Cosmetic Lenses from Various Manufacturers

# Motivation

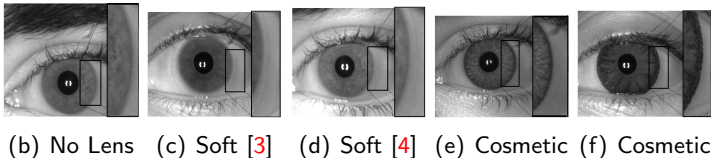
- Introduction of contact lens pose challenge in iris recognition
  - Help a criminal in evading detection
  - Create a synthetic identity
  - Impersonate a target identity



(a) Impersonation using contact lens

# Contribution

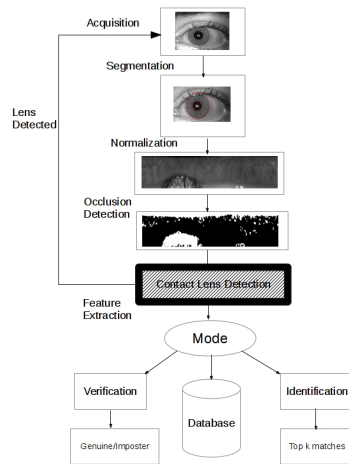
- Construction of a Contact Lens Iris Dataset
  - 50 subjects *ie.* 100 eye classes
  - Each subject in No Lens, Soft Lens and Cosmetic Lens class
  - 4 manufacturers for cosmetic and 2 for soft lenses
  - 12823 total images



# Contribution

- Quantifying effect of Soft and Cosmetic Contact Lens
  - Varying probe class keeping the gallery class same
  - In terms of  $D_{EER}$  and  $D_{CRR}$  ie degradation in Correct Recognition Rate and Equal Error Rate
- Detection of Cosmetic Contact Lens
  - Texture descriptor
  - Intensity variation along the boundary

# Contribution



# Database

- IITK Contact Lens Database

<b>Types of Contact Lens</b>	Cosmetic lens, Soft lens and no lens
<b>Cosmetic Lens Manu.</b>	CibaVision, Flaymboyent, Oxycolor , Freshlook [2]
<b>Cosmetic Lens Color</b>	Hazel,Green,Blue,Gray
<b>Soft Lens Manu.</b>	Johnson & Johnson [3], Bausch and Lomb [4]
<b>Iris Sensor</b>	Vista Imaging FA2 [5]
<b>Images per class</b>	C:4218, N:4551, Y:4054
<b>Min. images per eye class</b>	20
<b>Total Images</b>	12823

Table 1: IITK Contact Lens Dataset Summary

# Iris Preprocessing

- During segmentation, the acquired iris image is thresholded to obtain a binary iris image.
- Sobel operator is used to detect edges on the binary image itself.
- Pupil boundary is detected by applying an improved version of the standard hough transform [22, 23]. It makes use of the fact that an edge point  $(x, y)$  lies on a circle whose center is along the normal to the gradient direction  $\theta(x, y)$  at that point.
- The circular integro-differential operator is applied over two non-occluded sectors of the iris image. It finds the pupil center,  $c_p$ .

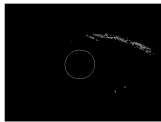
# Iris Preprocessing



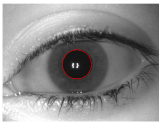
(a) Raw Iris



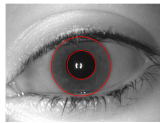
(b) Thresholded Image



(c) Edge Map



(d) Pupil Seg.



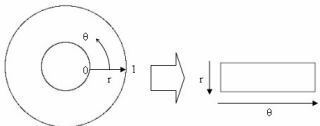
(e) Iris Seg.

Figure 5: Stages in Iris Preprocessing [22]

# Iris Preprocessing

- Eyelids, eyelashes, and specular reflections hide iris texture leading to unnecessary false matches.
- The two eyelids are centered around  $90^\circ$  and  $270^\circ$  with respect to horizontal direction in the normalized iris image. Region-growing is started with these two points as seeds to detect the entire eyelid area.
- Eyelashes are located using a feature vector combining the high local contrast of separable eyelashes and lower average intensity of multiple eyelashes.
- Final occlusion mask is obtained by logical OR-ing of the three individual binary masks for eyelids, eyelashes, and specular reflections [24].

# Iris Preprocessing



(a) Normalization



(b) Normalized Iris



(c) Occlusion Detection

Figure 6: Stages in Iris Preprocessing

# Effect of Contact Lens on Iris Recognition

- Template Matching
  - Fixed Gallery class ie. "No Lens" Class
  - Variable Probe class ie. No, Soft, Cosmetic
- Metrics
  - Correct Recognition Rate (Identification)

$$CRR = \frac{\sum_{i=1}^N EQUAL((\text{Best match}(i)), \text{Subject}(i))}{N} \times 100 \quad (1)$$

- Equal Error Rate(Verification)

$$FAR(t) = \frac{\text{Number of impostor falsely accepted as genuine}}{\text{Total number of impostor matchings}} \times 100 \quad (2)$$

$$FRR(t) = \frac{\text{Number of genuine falsely rejected as impostor}}{\text{Total number of genuine matchings}} \times 100 \quad (3)$$

# Effect of Contact Lens on Iris Recognition

- Irrespective of Technique and Database, there is decrease in CRR and increase in EER if a user is either wearing soft lens or cosmetic contact lens

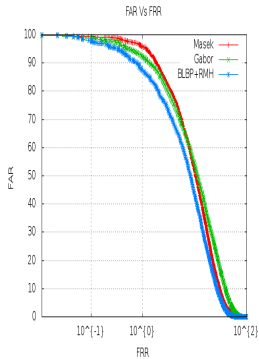
Dataset	Tech.	Masek[13]				Gabor[14]				BLBP+RMH[15]			
		GC-PC	CRR	D <sub>CRR</sub>	EER	D <sub>EER</sub>	CRR	D <sub>CRR</sub>	EER	D <sub>EER</sub>	CRR	D <sub>CRR</sub>	EER
IIITD Cogent [11, 12]	No-No	96.76	-	4.56	-	95.27	-	6.51	-	98.75	-	<b>3.14</b>	-
	No-Soft	96.25	0.51	5.41	0.85	92.75	2.52	6.49	0.02	97.50	1.25	<b>4.17</b>	1.03
	No-Cosmetic	57.03	39.73	<b>17.16</b>	12.60	35.92	59.35	23.80	17.29	68.34	30.41	18.43	15.29
IIITD Vista [11, 12]	No-No	99.75	-	2.27	-	99.75	-	2.35	-	100	-	<b>1.16</b>	-
	No-Soft	91.50	8.25	8.04	5.77	92.75	7.00	6.87	4.52	93.75	7.25	<b>5.31</b>	4.15
	No-Cosmetic	58.79	40.96	26.11	23.84	48.74	51.01	21.17	18.82	70.85	29.15	<b>12.62</b>	11.46
IITK	No-No	99.79	-	3.34	-	99.69	-	3.81	-	99.89	-	<b>1.43</b>	-
	No-Soft	95.00	<b>4.79</b>	7.36	4.02	95.59	4.10	7.99	4.18	96.66	3.23	<b>4.86</b>	3.43
	No-Cosmetic	66.81	32.98	21.31	17.97	52.50	47.19	24.54	20.73	67.38	32.51	<b>19.59</b>	18.16
Avg Degdn	No-Soft	-	4.51	-	3.54	-	4.54	-	2.90	-	3.91	-	2.87
	No-Cosmetic	-	37.89	-	18.13	-	52.51	-	18.94	-	30.69	-	14.97

GC and PC stand for gallery class and probe class respectively. CRR and EER in %

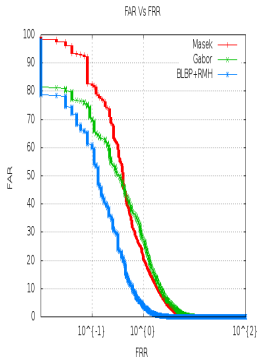
Table 2: Performance Degradation due to use of Contact Lens

# Experimental Results (IITK)

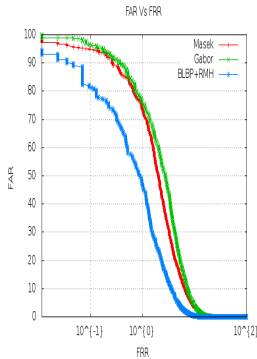
- ROC curves



(a) No-Cosmetic



(b) No-No

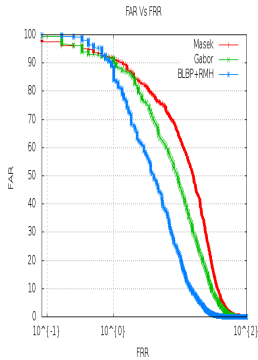


(c) No-Soft

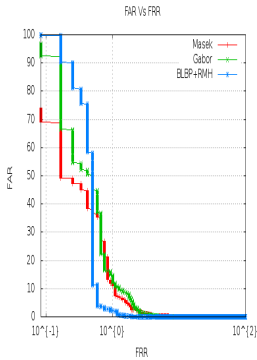
All the graphs use  $\log_{10}$  scale for X-axis

# Experimental Results (IIITD Vista)

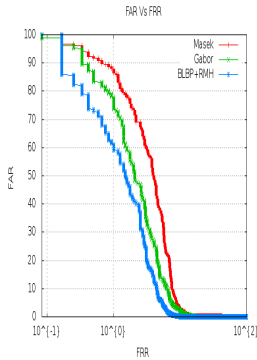
- ROC curves



(d) No-Cosmetic



(e) No-No

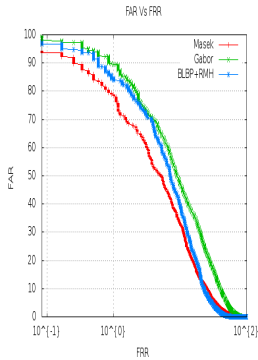


(f) No-Soft

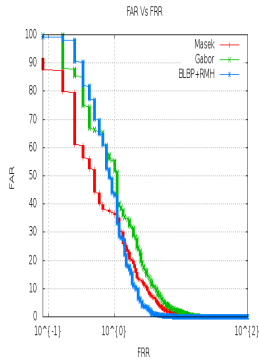
All the graphs use  $\log_{10}$  scale for X-axis

# Experimental Results (IIITD Cogent)

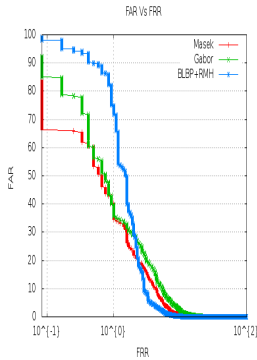
- ROC curves



(g) No-Cosmetic



(h) No-No

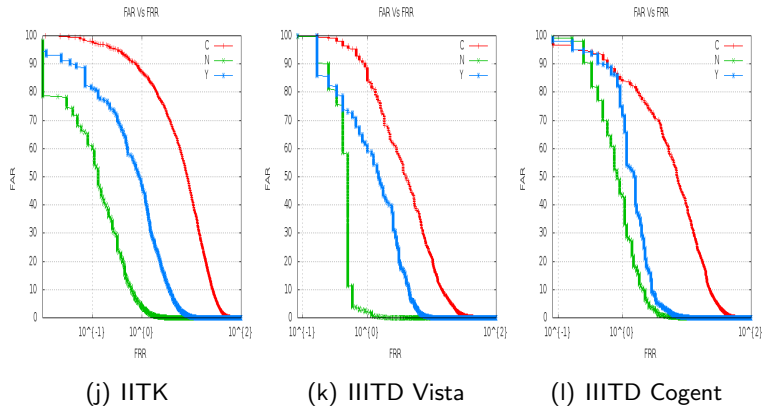


(i) No-Soft

All the graphs use  $\log_{10}$  scale for X-axis

# Experimental Results

- ROC curves



All the graphs use  $\log_{10}$  scale for X-axis

# Lens Detection

- Texture Descriptors

- Grey-Level Co-occurrence Matrix [17]
- Local Binary Patterns [16]
- Binary Statistical Image Features [18]
- Binary Gabor Patterns
- Local Phase Quantization



(m) No Lens



(n) Cosmetic Lens

Figure 7: Example Images with Soft Lens in IITK Dataset

## Binary Gabor Pattern [6]

- Texture Descriptor inspired by LBP
- Real and Complex part of Gabor filter

$$g(x, y) = \exp\left(-\frac{1}{2}\left(\frac{(x')^2}{\sigma^2} + \frac{(y')^2}{(\gamma\sigma)^2}\right)\right) \cos\left(\frac{2\pi}{\lambda}x'\right) \quad (4)$$

$$g(x, y) = \exp\left(-\frac{1}{2}\left(\frac{(x')^2}{\sigma^2} + \frac{(y')^2}{(\gamma\sigma)^2}\right)\right) \sin\left(\frac{2\pi}{\lambda}x'\right) \quad (5)$$

where  $x' = x \cos(\theta) + y \sin(\theta)$  and  $y' = -x \sin(\theta) + y \cos(\theta)$ ,  $\theta$  represents the orientation of the gabor filter with respect to normal,  $\gamma$  denotes the spatial aspect ratio ,  $\sigma$  denotes the sigma of Gaussian and  $\lambda$  is the wavelength of the sinusidal function.

# Binary Gabor Pattern [6]

- Gabor filter at 8 orientations
- Thresholded based on sign of response
- Binarized to obtain a vector
- Transformed to obtain a unique number

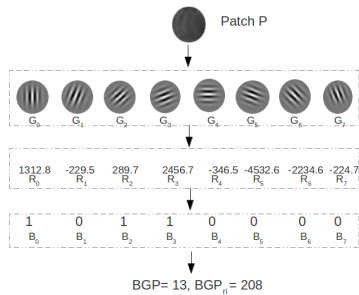


Figure 8: BGP value computation

## Binary Gabor Pattern [6]

- $2^7$  unique values are possible
- To make the descriptor rotation invariant

$$BGP = \sum_{i=0}^7 B_i \cdot 2^i \quad (6)$$

$$BGP_{ri} = \text{MAX}(RIGHTSHIFT(BGP, i) | i = 0..7) \quad (7)$$

- 36 unique values are possible
- 3 value pairs for  $\sigma$  and  $\lambda$  with a fixed  $\gamma$
- 216-bit descriptor

# Local Phase Quantization [7]

- Texture descriptor
- Robust to image blurring,
- PSF causing blur centrally symmetric
- Ideal Motion and Focus Blur PSF is rectangular [25]

$$I(x, y) = i(x, y) * b(x, y) \quad (8)$$

$$L(u, v) = I(u, v).B(u, v) \quad (9)$$

$$\angle L = \angle I + \angle B \quad (10)$$

- $B$  is represented by *sinc* function containing positive values before the zero-crossing

# Local Phase Quantization [7]

- 2D-frequencies  $[a, 0]$ ,  $[0, a]$ ,  $[a, a]$  and  $[a, -a]$  where  $a$  is a scalar less than zero-crossing
- Real and Complex responses from these four frequencies are concatenated to form a 8-bit vector
- Whitening Transform for decorrelation
- Quantized between values ranging from 0 to 255 using binary coding
- Histogram composed of the Quantized values

# Lens Detection Process

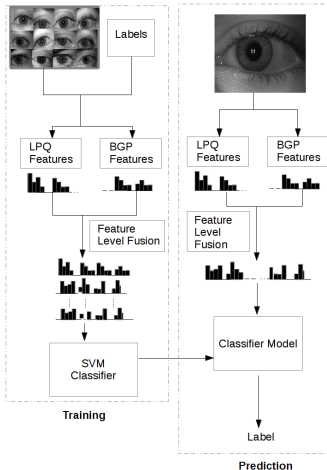


Figure 9: Lens Detection Process

# Experimental Results

- 256-bin histogram LPQ and 216-bin from BGP
- 472-bit descriptor
- 66% training and 33% testing
- SVM with RBF kernel as classifier

$$CCR = \frac{TP + TN}{TP + TN + FP + FN} \times 100 \quad (11)$$

$$FAR = \frac{FP}{TN + FP} \times 100 \quad (12)$$

Descriptor	GLCM[9]		LBP[10]		BSIF[8]		Our(LPQ+BGP)	
Dataset	CCR	FAR	CCR	FAR	CCR	FAR	CCR	FAR
Our dataset	57.05	30.02	97.54	0.55	98.44	<b>0.55</b>	<b>98.91</b>	0.86
IIITD Vista	50.00	55.88	99.70	0.58	99.70	0.58	<b>99.85</b>	<b>0.29</b>
IIITD Cogent	36.86	46.07	89.54	12.91	<b>98.21</b>	3.29	96.81	<b>2.82</b>
UND	56.59	31.11	95.82	6.22	85.93	28.44	<b>99.12</b>	<b>1.55</b>

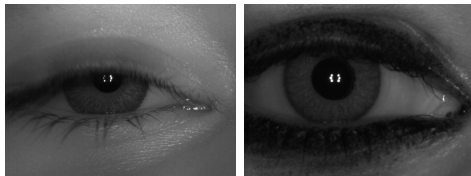
Table 3: CCR and FAR across Various Texture Description Techniques

# Experimental Results

- Blurred Images



Our Contact Lens dataset



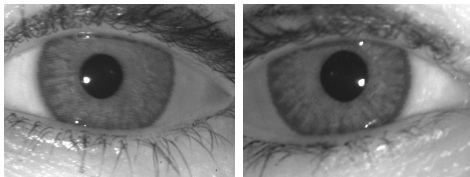
IIITD Vista Contact Lens dataset

# Experimental Results

- Blurred Images



IIITD Cogent Contact Lens dataset



ND\_2010 Contact Lens dataset

# Conclusion

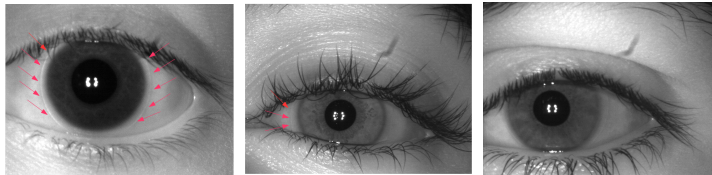
- Average  $D_{EER}$  for
  - soft lens is 3.10%
  - cosmetic lens is 17.32%
- Average  $D_{CRR}$  for
  - soft lens is 4.32%
  - cosmetic lens is 49.70%
- Average Detection
  - False Acceptance Rate of 1.38%
  - Correct Classification Rate of 98.92%

# Conclusion

- Three iris recognition techniques have been used to quantify and firmly establish the degradation of recognition performance both in the case of soft and cosmetic contact lens.
- Our technique outperformed LBP,GLCM and BSIF for IIITD Vista, IIITD Cogent and ND 2010 datasets.
- BSIF performed slightly better than BGP+LPQ over our dataset as there were four different cosmetic lens classes present in the dataset. However, our approach performs significantly better than BSIF for ND\_2010 dataset which contains blurred images

# Future Work

- Soft Lens
- Used change in intensity

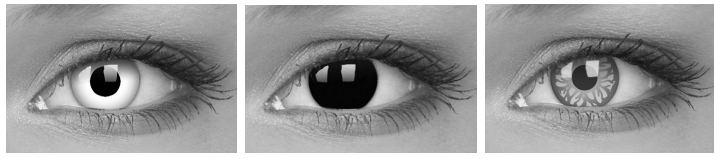


(a) Both Edges Visible (b) One edge Visible (c) No Edge Visible

Figure 12: Example Images with Soft Lens in IITK Dataset

# Future Work

- Unconventional Lenses
- Need for a texture independent approach
- Train on one, test on other db
  - Need a dataset such as we have in an antivirus
  - Ensemble of too many methods
  - Two classes vs One class



(a) All White

(b) All Black

(c) Hallowen Style

Figure 13: Unconventional Lenses Available in the Market [26]

Thanks

**Thank You.**

# References I

-  Flom, Leonard and Safir, Aran  
Google Patents  
*US Patent 4,641,349 (1987)*
-  Freshlook Contact Lenses  
<http://www.acuvue.co.in/>  
Accessed: 2014-12-1
-  Johnson and Johnson Acuvue Contact Lenses  
<http://www.acuvue.co.in/>  
Accessed: 2014-12-1
-  Bausch and Lomb Contact Lenses  
<http://www.bausch.in/our-products/contact-lenses/lenses-for-short-sighted-long-sighted/iconnect/>  
Accessed: 2014-12-1

## References II

-  Vista Imaging FA2 Sensor  
[http://www.vistaimaging.com/FA2\\_product.html](http://www.vistaimaging.com/FA2_product.html)  
Accessed: 2014-12-1
-  Zhang, Lin and Zhou, Zhiqiang and Li, Hongyu  
Binary gabor pattern: An efficient and robust descriptor for  
texture classification  
*Proc. 19th IEEE International Conference on Image Processing  
(ICIP) 81-84(2012)*
-  Ojansivu, Ville and Heikkilä, Janne  
Blur insensitive texture classification using local phase  
quantization  
*Image and signal processing 236-243(2008)*

## References III

-  Komulainen J, Hadid A Pietikinen M textured contact lens detection by extracting BSIF description from Cartesian iris images  
*Proc. International Joint Conference on Biometrics (IJCB 2014), Clearwater, FL (2014)*
-  Wei, Zhusi and Qiu, Xianchao and Sun, Zhenan and Tan, Tieniu  
Counterfeit iris detection based on texture analysis  
*Proc. 19th International Conference on Pattern Recognition, 1-4 (2008)*
-  He, Zhaofeng and Sun, Zhenan and Tan, Tieniu and Wei, Zhusi  
Efficient iris spoof detection via boosted local binary patterns  
*Advances in Biometrics 1080-1090 (2009)*

## References IV

-  Kohli, Naman and Yadav, Daksha and Vatsa, Mayank and Singh, Richa  
Revisiting iris recognition with color cosmetic contact lenses  
*Proc. International Conference on Biometrics (ICB)* pp. 1-7 (2013)
-  Yadav, Daksha and Kohli, Naman and Doyle, JS and Singh, Richa and Vatsa, Mayank and Bowyer, Kevin W  
Unraveling the Effect of Textured Contact Lenses on Iris Recognition  
*Proc. IEEE Transactions on Information Forensics and Security* (2014)
-  Masek, L.  
Recognition of human iris patterns for biometric identification  
*M.Tech Thesis, The University of Western Australia* pp. 33-36 (2003)

## References V

-  Daugman, J.  
How iris recognition works.  
*In: International Conference on Image Processing (ICIP).* pp. 33-36 (2002)
-  Nigam, Aditya and Krishna G, Vamshi and Gupta, Phalguni  
Iris Recognition Using Block Local Binary Patterns and  
Relational Measures  
*In: Proceeding of International Joint Conference on Biometrics*  
pp. 1-7(2014)
-  Ojala, Timo and Pietikäinen, Matti and Mäenpää, Topi  
Multiresolution Gray-Scale and Rotation Invariant Texture  
Classification with Local Binary Patterns  
*IEEE Transactions on Pattern Analysis and Machine  
Intelligence.* pp. 971-987 (2002)

## References VI

-  Haralick, Robert M and Shanmugam, Karthikeyan and Dinstein, Its' Hak  
Textural features for image classification  
*In: IEEE Transactions on Systems, Man and Cybernetics pp. 1363-1366 (1973)*
-  Kannala, Juho and Rahtu, Esa  
Bsif: Binarized statistical image features  
*In: Proc. 21st International Conference on Pattern Recognition (ICPR) pp. 1363-1366 (2012)*
-  Heikkilä, Marko and Pietikäinen, Matti and Schmid, Cordelia.  
Description of interest regions with local binary patterns.  
*Pattern Recognition. 42(3), 425-436 (2009)*

## References VII

-  Ojala, Timo and Pietikäinen, Matti and Mäenpää, Topi.  
Multiresolution Gray-Scale and Rotation Invariant Texture  
Classification with Local Binary Patterns.  
*IEEE Transactions on Pattern Analysis and Machine  
Intelligence.* 24(7), 971-987 (2002)
-  Comaniciu, Dorin and Ramesh, Visvanathan and Meer, Peter.  
Kernel-Based Object Tracking.  
*IEEE Transactions on Pattern Analysis and Machine  
Intelligence.* 25(5), 564-575 (2003)
-  Bendale, Amit and Nigam, Aditya and Prakash, Surya and  
Gupta, Phalguni.  
Iris Segmentation Using Improved Hough Transform.  
*In: Emerging Intelligent Computing Technology and  
Applications, Communications in Computer and Information*

## References VIII

*Science, vol. 304, pp. 408-415. Springer Berlin Heidelberg (2012)*

-  Nigam, Aditya and Gupta, Phalguni.  
Iris recognition using consistent corner optical flow.  
*In: Proceedings of the 11th Asian conference on Computer Vision - Volume Part I. pp. 358-369. ACCV'12, Springer-Verlag, Berlin, Heidelberg (2013)*
-  Bendale, Amit.  
Iris Recognition using Relational Measures.  
*M.Tech Thesis, Indian Institute of Technology Kanpur (2012)*
-  Banham, Mark R and Katsaggelos, Aggelos K  
Digital image restoration  
*IEEE Signal Processing Magazine 24-41(1997)*

# References IX

 Eyesbright Inc  
<http://www.eyesbright.com>  
Accessed: 2014-11-05

# Sobel Operator

- The Sobel operator uses two kernels of dimension  $3 \times 3$  to obtain vertical and horizontal gradients of an image.
- The derivatives resulting from convolving the kernels with the image approximate the exact gradient of pixels.

$$G_v = \begin{bmatrix} +1 & +2 & +1 \\ 0 & 0 & 0 \\ -1 & -2 & -1 \end{bmatrix} * I \quad G_h = \begin{bmatrix} +1 & 0 & -1 \\ +2 & 0 & -2 \\ +1 & 0 & -1 \end{bmatrix} * I$$

where '\*' stands for the convolution operator. It is assumed that the x-coordinate (vertical direction) increases downwards while the y-coordinate (horizontal direction) increases from left to right.

# Sobel Operator

- The gradient direction at a pixel is given by Equation 13.
- Positive value of  $\theta(x, y)$  indicates that the pixel lies on an edge created by a light to dark transition; otherwise its value is negative.

$$\theta(x, y) = \tan^{-1} \left( \frac{G_v(x, y)}{G_h(x, y)} \right) \quad (13)$$

# Hough Transform

- Approximate circular shape detection for a particular radius can be formulated as:

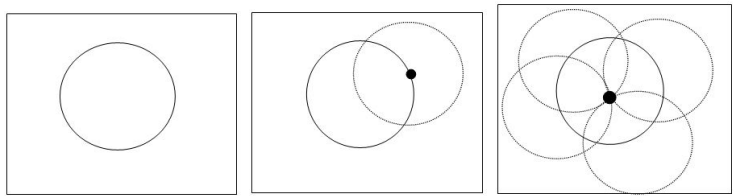
$$V(a, b) = |\{(x, y) \in E : (x - a)^2 + (y - b)^2 = R^2\}| \quad (14)$$

$$(x_c, y_c) \leftarrow \operatorname{argmax}_{(a,b)}(V) \quad (15)$$

where  $E$  is the edge map on which the circle is to be detected,  $(a, b)$  is the candidate center of circle and  $V(a, b)$  is its votes.

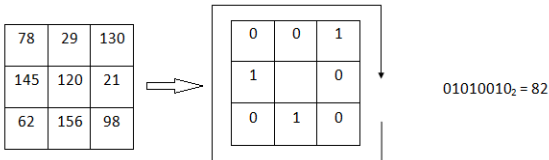
- Iris inner and outer boundaries are approximate circles.
- Standard circular Hough transform does exhaustive search on all candidate circles to find actual circle.

# Standard Hough Transform



- (a) Edge map of image (b) For an edge point, (c) Candidate with  
locus of possible center maximum votes is the  
actual center

Figure 14: Standard Circular Hough Transform

Figure 15: *LBP* value computation

- The basic *LBP* operator [20] consists of thresholding the eight neighbours of a central pixel by its value followed by creating a decimal representation of the binary string.
- Every  $3 \times 3$  neighbourhood gives a value between 0 to 255, called the *LBP* value.
- It corresponds to a texture pattern which can be used as a feature representing the spatial structure.

# Grey Level Co-occurrence Matrix

- A matrix that defines the distribution of co-occurring values at a given offset
- Denoted by :-

$$C_{\Delta x, \Delta y}(i, j) = \sum_{p=1}^{n} \sum_{q=1}^{m} \begin{cases} 1, & \text{if } I(p, q) = i \text{ and } I(p + \Delta p, q + \Delta q) = j \\ 0, & \text{otherwise} \end{cases} \quad (16)$$

where  $n \times m$  denotes the dimensions of image,  $(x, y)$  are intensity values,  $(p, q)$  is the position of a particular pixel and  $(\Delta p, \Delta q)$  is the offset.

## Grey Level Co-occurrence Matrix

$$I = \begin{bmatrix} 0 & 2 & 3 & 1 \\ 1 & 3 & 0 & 2 \\ 1 & 0 & 3 & 2 \\ 2 & 1 & 3 & 2 \end{bmatrix} \quad G = \begin{bmatrix} (0,0) & (0,1) & (0,2) & (0,3) \\ (1,0) & (1,1) & (1,2) & (1,3) \\ (2,0) & (2,1) & (2,2) & (2,3) \\ (3,0) & (3,1) & (3,2) & (3,3) \end{bmatrix}$$

$$G_0(I) = \begin{bmatrix} 0 & 1 & 2 & 2 \\ 1 & 0 & 1 & 3 \\ 2 & 1 & 0 & 3 \\ 2 & 3 & 3 & 0 \end{bmatrix} \quad G_{90}(I) = \begin{bmatrix} 0 & 2 & 0 & 3 \\ 2 & 2 & 2 & 0 \\ 0 & 2 & 4 & 1 \\ 3 & 0 & 1 & 2 \end{bmatrix}$$

$$G_{45}(I) = \begin{bmatrix} 2 & 0 & 1 & 0 \\ 0 & 0 & 1 & 2 \\ 1 & 1 & 0 & 2 \\ 0 & 2 & 2 & 2 \end{bmatrix} \quad G_{135}(I) = \begin{bmatrix} 0 & 1 & 1 & 2 \\ 1 & 2 & 0 & 0 \\ 1 & 0 & 0 & 1 \\ 2 & 0 & 1 & 2 \end{bmatrix}$$

- Certain patterns are regarded as *uniform* because there are very few bit transitions in their binary representation.
- It has been experimentally shown that these uniform patterns constitute most of the natural  $3 \times 3$  patterns found in surface textures.

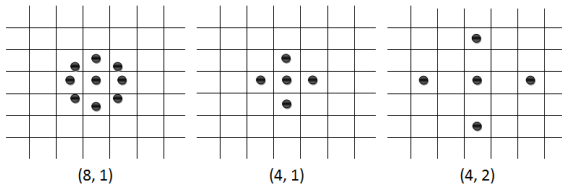


Figure 16: Circularly symmetric LBP neighbourhoods for different ( $n, d$ )

- Different circularly symmetric neighbour sets can be chosen for a central pixel  $c_p$ .

# Gabor filters

- Gabor filters are believed to be particularly suited for random texture representation (like iris.)
- 2-D Gabor filters:

$$G(x, y) = e^{-\pi \left[ \frac{(x-x_0)^2}{\alpha^2} + \frac{(y-y_0)^2}{\beta^2} \right]} \cdot e^{-2\pi i [u_0(x-x_0) + v_0(y-y_0)]} \quad (17)$$

where  $(x_0, y_0)$  is the position in the image  $I$ ,  $(\alpha, \beta)$  specify the effective length and width, and  $(u_0, v_0)$  specify modulation which has frequency  $\omega_0 = (u_0^2 + v_0^2)^{\frac{1}{2}}$  and orientation  $\theta_0 = \tan^{-1} \left( \frac{v_0}{u_0} \right)$ .

## Gabor Filters cntd..

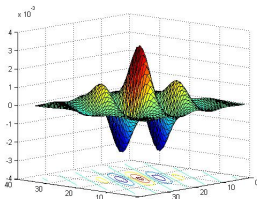
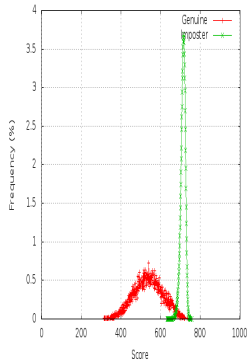


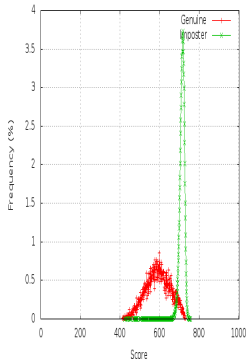
Figure 17: Gabor filter with  
 $\alpha = 7, \beta = 7, u_0 = v_0 = 0.1, (x_0, y_0) = (20, 20)$

- This filter is convolved with image.
- The sign of real and imaginary parts of output decide the 2-bit encoding for each pixel (00,01,10,11) based on the quadrant.
- The output bits are concatenated spatially to generate the "IrisCode".

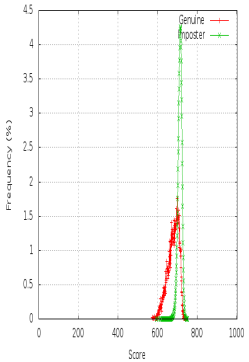
# Genuine Imposter Plots (IITK)



(a) No-No

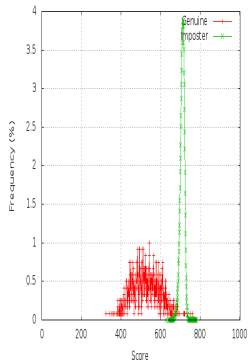


(b) No-Soft

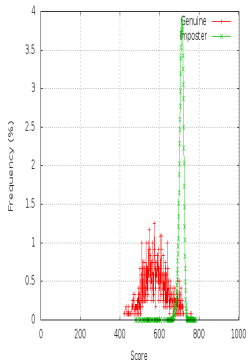


(c) No-Cosmetic

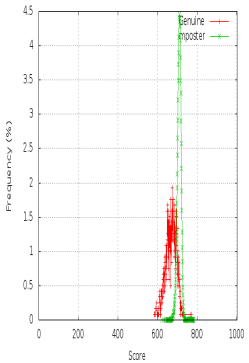
# Genuine Imposter Plots (IIITD Vista)



(d) No-No

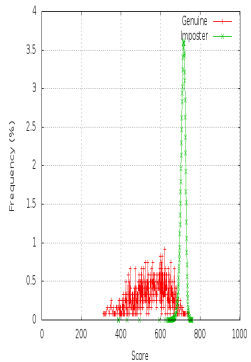


(e) No-Soft

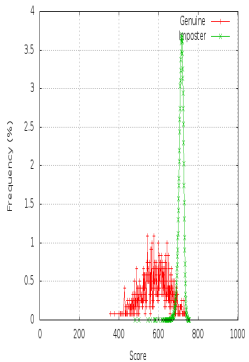


(f) No-Cosmetic

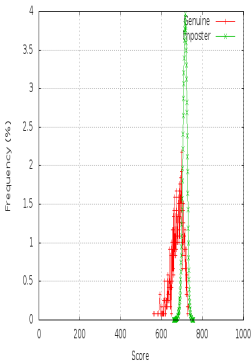
# Genuine Imposter Plots (IIITD Cogent)



(g) No-No



(h) No-Soft



(i) No-Cosmetic

# Experimental Results

- GLCM - Mean and Range of
  - Contrast
  - Correlation
  - Sum Average
  - Sum Entropy
- LBP
  - $LBP_{8,1}^{riu2}$  and  $LBP_{16,2}^{riu2}$
- BSIF
  - Radius of features learnt - 3
  - Size of features learnt - 12 bits
- BGP
  - $(1.3, 0.7), (5.2, 2.5)$  and  $(22, 4.5)$  as  $(\lambda, \sigma)$  pair